

SUPPLEMENTAL DATA FOR:

Histone deacetylase inhibition prevents the growth of primary and metastatic osteosarcoma

Jeremy J. McGuire, Niveditha Nerlakanti, Chen Hao Lo, Marilena Tauro, T.J. Utset-Ward, Damon Reed⁴ and Conor C. Lynch

Table of Contents:

Supplemental Materials and Methods.....	page 2
Supplemental Table S1.....	page 3
Supplemental Figure S1.....	page 4
Supplemental Figure S2.....	page 5
Supplemental Figure S3.....	page 6
Supplemental Figure S4.....	page 7
Supplemental Figure S5.....	page 8
Supplemental References.....	page 9

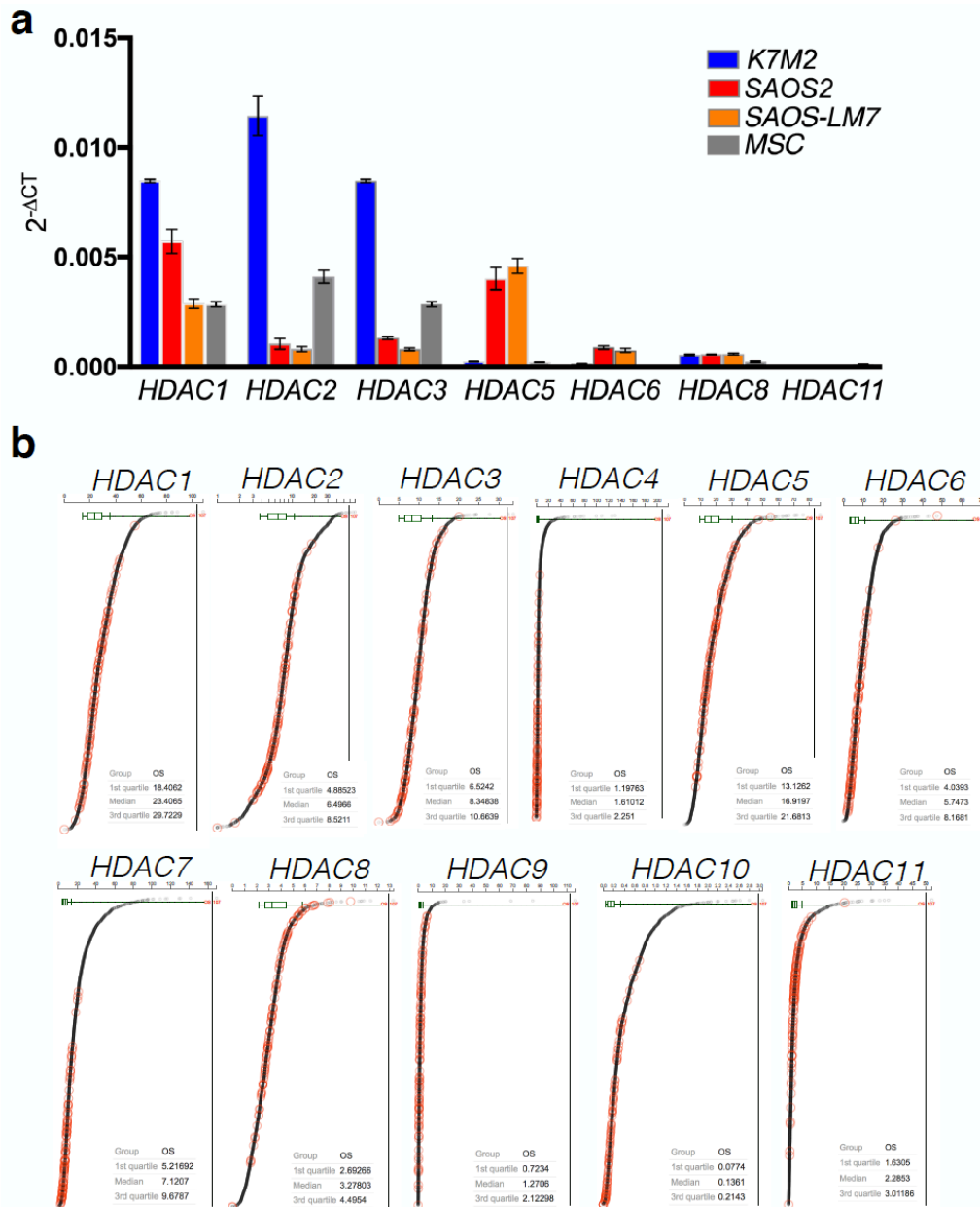
Supplementary Materials and Methods:

All materials and methods used for supplemental data are described in the main manuscript.

Supplemental Table S1. Human and mouse HDAC primers for qRT-PCR analysis

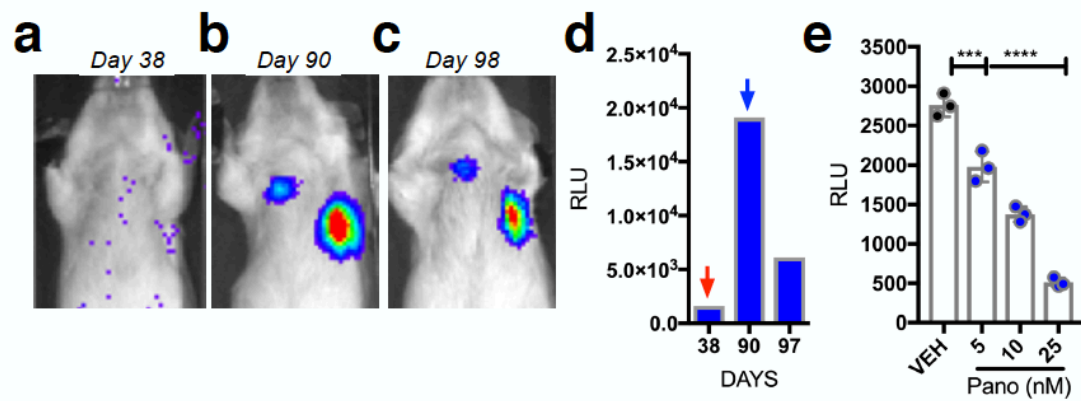
TARGET	HUMAN	MOUSE
<i>HDAC 1</i>	5'-GGTCCAAATGCAGGCGATTCCT-3' 3'-TCGGAGAACTCTTCCTCACAGG-5'	5'-TGAAGCCTCACCGAATCCGCAT-3' 3'-TGGTCATCTCCTCAGCATTGGC-5'
<i>HDAC 2</i>	5'-CTCATGCACCTGGTGTCCAGAT-3' 3'-GCTATCCGCTTGTCTGATGCTC-5'	5'-GTTTTGTCAGCTCTCCACGGGT-3' 3'-CTTGGCATGATGTAGTCTCCAG-5'
<i>HDAC 3</i>	5'-GAGTTCTGCTCGCGTTACACAG-3' 3'-CGTTGACATAGCAGAAGCCAGAG-5'	5'-AACCTCATCGCCTGGCATTGAC-3' 3'-GTAGTCTCAGAATGGAAGCGG-5'
<i>HDAC 5</i>	5'-CGCTGAGAATGGCTTTACTGGC-3' 3'-GTGTAGAGGCTGAACTGGTTGG-5'	5'-ACCAGCAGTTCCTGGAGAAGCA-3' 3'-TCCGTCAGCTCCTCTTCTGTCT-5'
<i>HDAC 6</i>	5'-GCCTCAATCACTGAGACCATCC-3' 3'-GGTGCCTTCTTGGTGACCAACT-5'	5'-TCGCTGTCTCATCCTACCTGCT-3' 3'-GTCAAAGTTGGCACCTTCACGG-5'
<i>HDAC 8</i>	5'-TGTGCTGAAATCACGCCAAGC-3' 3'-ACCACTCCTCAGCTCTGGAAC-5'	5'-GTCAGCCAAGAAGGTGATGAGG-3' 3'-ACACTTCCCGTCAATCAGGCAC-5'
<i>HDAC 11</i>	5'-CTTCTGTGCCTATGCGGACATC-3' 3'-GAAGTCTCGCTCATGCCATTG-5'	5'-AAGGCATCTCCAGAGCCACCAT-3' 3'-CAGGGTAGATGTGGCGGTTGTA-5'
<i>Actin</i>	5'-CACCATTGGCAATGAGCGGTTTC-3' 3'-AGGTCTTTGCGGATGTCCACGT-5'	5'-CATTGCTGACAGGATGCAGAAGG-3' 3'-TGCTGGAAGGTGGACAGTGAGG-5'

Supplemental Figure S1



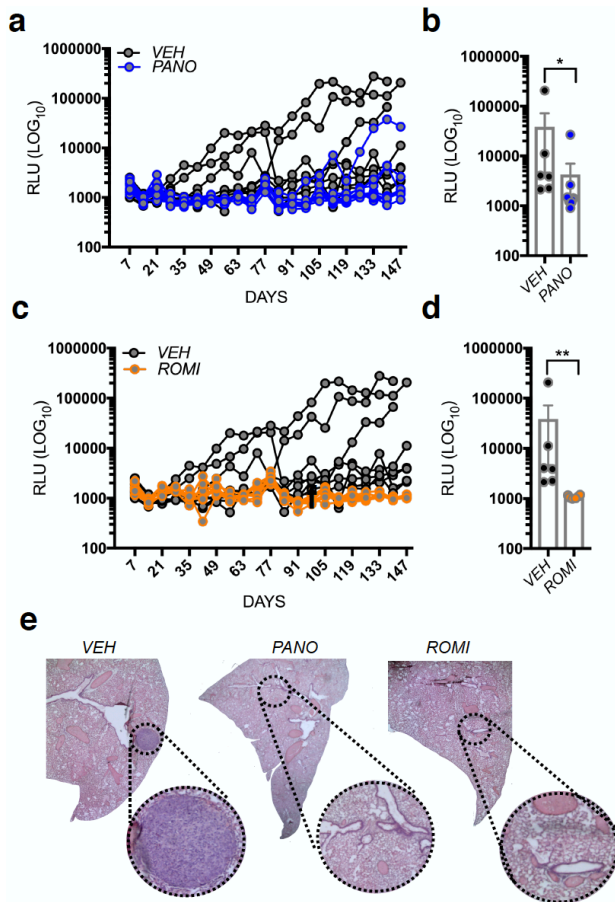
Supplemental Fig. S1. HDAC expression in osteosarcoma cell lines and osteosarcoma patient specimens. a. qRT-PCR analysis of HDAC gene expression in human and mouse osteosarcoma cell lines. Gene expression for each HDAC examined target is normalized to the actin levels for each cell line and graphed as $2^{-\Delta CT}$. **b.** Analysis of HDAC gene expression (RNA-Seq) osteosarcoma (OS) patients (n=107). Data is shown fragments per kilobase million (FPKM) and generated from the St. Jude PeCan database (<https://pecan.stjude.cloud/proteinpaint/>) (1).

Supplemental Figure S2



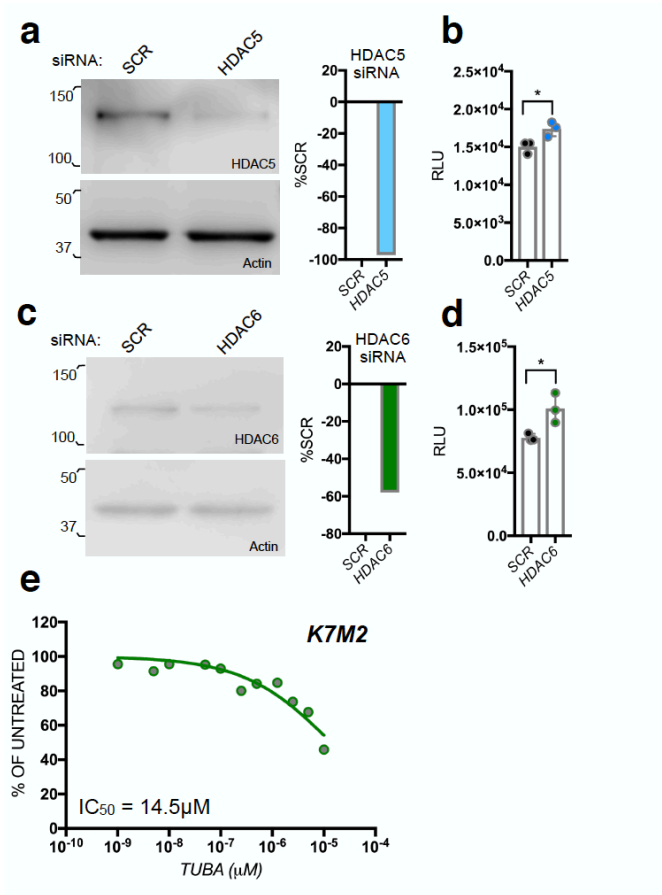
Supplemental Fig. S2. Panobinostat retreatment reduces outgrowing lung metastatic osteosarcoma. a-d. Bioluminescent (RLU) analysis of K7M2 lung metastatic growth in mouse #23 treated with panobinostat until day 38 (a) when treatment ceased. At day 90, panobinostat treatment was reinitiated (b) with subsequent imaging at day 97 (c). Bioluminescent (RLU) values are shown for each point (d). Treatment cessation and initiation are indicated by red and blue arrows respectively. **e.** Metastatic K7M2 cells isolated from lung tissue were treated with Panobinostat over 24 hours and the impact on growth (RLU) determined.

Supplemental Figure S3



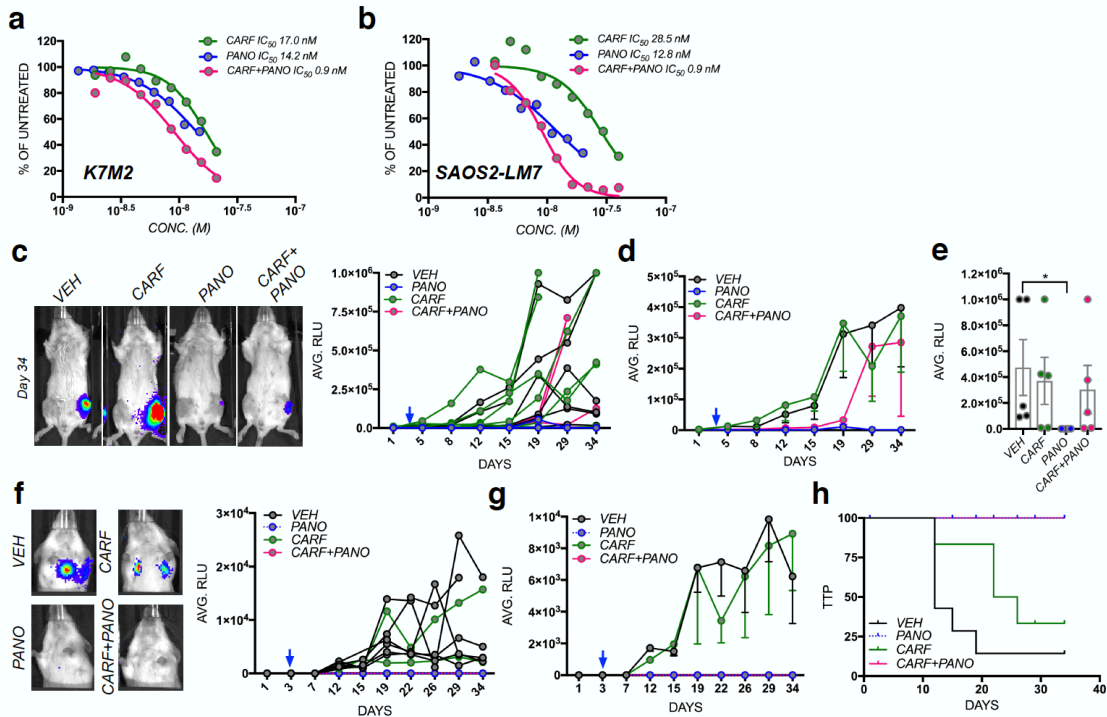
Supplemental Fig. S3. Panobinostat and romidepsin significantly impact the growth of established lung metastatic SAOS-LM7 osteosarcoma. **a, b** Spider plot (**a**) of SAOS-LM7 bioluminescence over time in individual vehicle control (*VEH*; n=8) or panobinostat (*PANO*; n=9) treated mice. Treatment was initiated seven days post inoculation of the osteosarcoma cells. Tumor volumes based on bioluminescence (RLU) were compared at day 147 (**b**). **c, d** Spider plot (**a**) of SAOS-LM7 bioluminescence over time in individual vehicle control (*VEH*; n=8) or romidepsin (*ROMI*; n=9) treated mice. Treatment was initiated seven days post inoculation of the osteosarcoma cells. Tumor volumes based on bioluminescence (RLU) were compared at day 147 (**d**). **e**. Representative H&E stained lung sections derived from vehicle control, panobinostat and romidepsin treated mice. Asterisks denotes statistical significance (* $p < 0.05$; ** $p < 0.01$).

Supplemental Figure S4



Supplemental Fig. S4. HDAC5 and 6 suppress osteosarcoma growth. **a, b.** Analysis of HDAC5 levels in K7M2 cells 24 hours subsequent to siRNA silencing (**a**) compared to scrambled control siRNA (SCR). Actin was used as a positive loading control. Numbers indicate molecular weight (kDa). Densitometry graphs illustrate the impact of silencing on HDAC5 levels. The effect of HDAC5 silencing on cell growth (**b**) was determined by measuring bioluminescence (RLU). **c, d.** Analysis of HDAC6 levels in K7M2 cells 24 hours subsequent to siRNA silencing (**c**) compared to scrambled control siRNA (SCR). Actin was used as a positive loading control. Numbers indicate molecular weight (kDa). Densitometry graphs illustrate the impact of silencing on HDAC5 levels. The effect of HDAC6 silencing on cell growth (**d**) was determined by measuring bioluminescence (RLU). **e.** The effects of the HDAC6 selective inhibitor tubastatin at varying concentrations on K7M2 viability over 24 hours.

Supplemental Figure S5



Supplemental Fig. S5. Carfilzomib has no effect on primary osteosarcoma growth or lung metastasis *in vivo*.

a, b. K7M2, and SAOS2-LM7 cell lines were incubated with the indicated concentrations of panobinostat (PANO), carfilzomib (CARF) or panobinostat plus carfilzomib (CARF+PANO) for 48 hr. Cell viability (CellTiter blue) is presented as a percentage of vehicle control.

c. Spider plot of K7M2 bioluminescence (RLU) over time in individual vehicle control (VEH; n = 6) carfilzomib (CARF; n = 7), panobinostat (PANO; n=6) or carfilzomib and panobinostat (CARF+PANO; n = 5) treated mice. Treatment was initiated 3 days subsequent to inoculation (blue arrow). Mice were removed from study upon reaching 1×10^6 relative light units (RLU). Representative images show bioluminescence in each group at day 34 with hotter colors indicating greater tumor burden.

d. Average of bioluminescence in vehicle control and treated mice.

e. Analysis of bioluminescence between the groups at day 34.

f. Spider plot of K7M2 lung bioluminescence (RLU) over time in individual mice from each group. Representative images show bioluminescence in each group at day 34. Lung bioluminescence was observed by blocking tibia signal with light proof material.

g. Analysis of average bioluminescence in spontaneous metastases arising from orthotopic

primary K7M2 tumors. **h.** Kaplan Meier curve of time to progression (TTP) of lung bioluminescence detection in mice bearing primary (tibial) K7M2 tumors in each group. Asterisks denotes statistical significance (* $p < 0.05$).

Supplemental References

1. Zhou X, Edmonson MN, Wilkinson MR, Patel A, Wu G, Liu Y, Li Y, Zhang Z, Rusch MC, Parker M, Becksfort J, Downing JR, Zhang J. Exploring genomic alteration in pediatric cancer using ProteinPaint. *Nat Genet.* 2016;48(1):4-6. doi: 10.1038/ng.3466. PubMed PMID: 26711108; PMCID: PMC4892362.